Percolation properties of random ellipses

W. Xia* and M. F. Thorpe
Department of Physics and Astronomy, Michigan State University, East Lansing, Michigan 48824
and Center for Fundamental Materials Research, Michigan State University,
East Lansing, Michigan 48824
(Received 31 August 1987)

We compute the percolation concentration for identical ellipses with aspect ratio b/a in a two-dimensional plane where both the centers and orientations are random. We have obtained a comprehensive set of results ranging from circles to needles which can be well fit by the interpolation formula $p_c=(1+4y)/(19+4y)$, where $y=b/a+a/b$. We also obtain results for random centers and random orientations along the two principal directions which are virtually indistinguishable from the previous case. These results are used to critique the various effective-medium theories that have been developed for the electrical conductance and elastic moduli of sheets containing random elliptical inclusions. An interpolation formula is developed that appears superior to all these effective-medium theories.

I. INTRODUCTION

The universal behavior of the critical exponents that describe transport quantities such as electrical conductivity, thermal conductivity, the diffusion constant, and elastic moduli of a composite system near the percolation threshold can be understood by continuum percolation theory.[1] Experimental results agree well with the theoretical predictions of such quantities.[2] In designing composite materials it is more important to know the *overall behavior* of the properties of these materials which are governed by nonuniversal quantities away from the critical region. The location of the critical point is also nonuniversal. When the concentration of one of the components (for simplicity, we will consider only two-component composite systems) is extremely low, the behavior of quantities like the electrical conductance can be adequately described by the Clausius-Mossotti equation.[3] In between these two extremes, an exact microscopic theory or detailed computer modeling of the transport properties would be very difficult and neither is currently available. Some progress has been made recently in studying two elliptical holes in a homogeneous medium.[4] However, even here there are still unresolved problems associated with overlapping inclusions that have prevented a useful generalization of the Clausius-Mossotti equations. Computer simulations have also not been possible because even the largest available machines cannot store enough information to meaningfully discretize such continuum systems. Thus a major research tool that has led to so much of our understanding of the response of discrete lattice systems[5] has not been available or exploited yet in continuum systems.

The purpose of this paper is to develop a semiphenomenological description of the behavior of the transport properties of these systems. Many effective-medium theories (EMT) have been developed[3,6–11] but are of dubious validity away from the dilute limit, where all these theories agree. In order to ascertain which of these theories are good for all concentrations, we have located the *critical concentration of randomly positioned ellipses at percolation.* These results are new except for the special case of circles and provide a most stringent test of effective-medium theories. We find that there are *no* reasonable EMT for electrical conductance; all fail to predict the correct critical concentration for circles. On the other hand, we find one such existing theory to be clearly superior and adequate for elastic inclusions. This is the asymmetric reinforced model (also called *SC A-A*, reinforced problem in Sec. II B of Thorpe and Sen).[7] This was originally derived for circular inclusions by Hill, Budiansky, Wu, and Berryman[8–10] using different self-consistent methods. In the circular limit symmetric and asymmetric theories are identical. Those results were generalized by Thorpe and Sen[7] to ellipses for which symmetric and asymmetric theories are no longer identical. Note, however, that this theory applies when the *circular inclusions are infinitely hard* so that the elastic compliance and not the elastic modulus vanishes at the critical concentration. We would expect that this effective-medium theory should also be superior for mixtures where the elliptical inclusions are hard. The *SC A-A* for holes does not give a good value for the critical concen-good value for the critical concentration.

The interpolation formula we develop incorporates the behavior at the two extremes (i.e., low concentrations and near the percolation threshold) for a system containing randomly distributed insulating elliptical laminae (i.e., holes) embedded in the uniform background of a conducting matrix.

The layout of this paper is as follows. In Sec. II we discuss the geometric aspects of continuum percolation for a system containing random elliptical laminae and in Sec. III we present our computer simulations of the percolation thresholds and compare with the results of previous work. In Sec. IV we use our results to *critique effective-medium theories* by examining their predictions for the percolation concentration. In Sec. V an interpolation formula for the electrical conductance is developed.

II. CONTINUUM PERCOLATION OF ELLIPTICAL LAMINAE

In continuum percolation, as well as in percolation on a lattice, an important quantity to describe the onset of

percolation is the percolation threshold p_c.[12] There exist extensive studies[13] in the literature of p_c for percolation on various lattices, where p_c is the fraction of bonds or sites remaining, depending on the type of percolation being studied. In the continuum percolation problem, p_c is defined to be the *fractional area* occupied by one phase which, in our case is the area *remaining* after the elliptical holes are removed. Figure 1 shows an example of the system under study and the area covered by ellipses has fractional area $1-p$ (at the percolation threshold $p=p_c$). Imagine that a constant voltage is applied across a conducting sheet and randomly oriented elliptical holes with random centers are punched out. As more and more material is removed, electric current flow through the sheet is restricted and vanishes at p_c. We are interested in how p_c changes as the geometry (i.e., aspect ratio) of one phase changes[14,15] or more precisely how p_c changes as the inclusions change from circles to needles. We use the *aspect ratio* b/a to describe the asymmetry of the ellipse where a and b (with $a>b$) are the major and minor semiaxes, respectively. Note that the *eccentricity of the ellipse is given by* $e=[1-(b/a)^2]^{1/2}$.

In the following discussion, identical, but randomly centered holes each with area A are removed from a two-dimensional $L\times L$ sheet. At hole concentration n per unit area, and *remaining area fraction* p, if we increase the hole density, then the area that is still available to be removed is pL^2. Therefore the *additional* area removed by changing the hole density from n to $n+dn$ is $pL^2A\,dn$. On the other hand, the area remaining is reduced to $pL^2-(p+dp)L^2$, so

$$pL^2-(p+dp)L^2=pL^2A\,dn\ ,$$

i.e.,

$$dp/p=-Adn\ ,$$

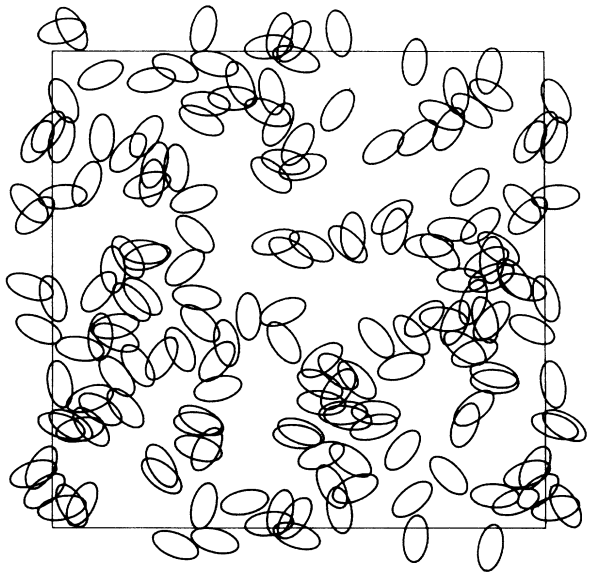

FIG. 1. An example of randomly oriented ellipses with aspect ratio $b/a=0.5$. The periodic boundaries can clearly be seen. Actual samples used were much larger.

so that

$$p=\exp(-An)\ , \tag{1}$$

where we note that $p=1$ when $n=0$ and $p=0$ when $n=\infty$. This formula has been used previously for circles[16,17] but is true for all shapes if sufficient randomness is present.[18] This is because the repeated random placement of an additional object or hole serves as a measure of the remaining area. We are, of course, always thinking of the thermodynamic limit when the system size is very large. Equation (1) can be generalized to three dimensions, where A is replaced by the volume of each individual hole and n is the hole density per unit volume (this can be visualized as Swiss cheese). In the two-dimensional case we are studying, $A=\pi ab$ and at the percolation threshold $n=n_c$; therefore,

$$p_c=\exp(-\pi abn_c)\ . \tag{2}$$

Equation (2) allows an immediate determination of the percolation threshold p_c for a given a and b once n_c is known or vice versa. This equation is very convenient to use in practice as it only involves counting; no area evaluation is involved. For *circles* we find from our simulations that

$$p_c=\exp(-\pi a^2n_c)=0.33\pm0.02\ , \tag{3}$$

where a is the circle radius and n_c is the density of circles per unit area at percolation. We have given generous error bars on (3). Our result (3) agrees well with other results for circles.[19] We also notice that a careful finite-size scaling study gives better results,[19] but this would need huge amounts of computer time if it were to be done for all aspect ratios. Our purpose here is to look at the general trend of how p_c changes with b/a.

In 2D the background ceases to percolate when the inclusions percolate. This is because there is no way *around* the infinite cluster. Therefore, there is a single percolation concentration. In higher dimensions, this is obviously not the case and there are two separate percolation concentrations for the inclusions and the backgrounds.

In continuum percolation involving identical objects, it is useful to introduce the *average excluded area* denoted as $\langle a_{ex}\rangle$.[20,21] For given relative orientations of two identical objects the *excluded area* is defined as the area that if the center of one is outside it, the two objects have no overlap at all. *Average* means over all allowed relative orientations. The excluded area at percolation is defined as

$$\langle A_{ex}\rangle=n_c\langle a_{ex}\rangle\ . \tag{4}$$

Although the mean-coordination number and the critical area or volume fraction are essentially invariant[22] in bond and site lattice percolation, respectively, $\langle A_{ex}\rangle$ is not quite such a quasiuniversal invariant quantity, and it has a small range.[12] Our results will be discussed in detail in Sec. III but we see from Table I that for randomly oriented ellipses,

$$3.4\le\langle A_{ex}\rangle\le4.5\ . \tag{5a}$$

TABLE I. Values of p_c, n_c, k, and $\langle A_{ex} \rangle$ are listed for *randomly oriented ellipses* for various aspect ratios b/a. The value of k is obtained by evaluating the perimeter s of the ellipse from an elliptic integral and using the formula in the text. The value of n_c is obtained from the simulation with the area of the ellipse fixed at $\pi/8$ and then $\langle A_{ex} \rangle$ is obtained from formulas (4) and (6). The error bar in $\langle A_{ex} \rangle$ is ± 0.2.

b/a	p_c	n_c	k	$\langle A_{ex} \rangle$
1.0000	0.33	2.8	1.000	4.4
0.9000	0.33	2.8	1.002	4.4
0.8000	0.33	2.8	1.009	4.4
0.7000	0.34	2.8	1.024	4.5
0.6000	0.35	2.7	1.050	4.5
0.5000	0.37	2.5	1.094	4.3
0.4000	0.41	2.3	1.171	4.2
0.3333	0.44	2.10	1.254	4.1
0.2500	0.50	1.76	1.432	4.0
0.2000	0.54	1.57	1.618	4.0
0.1500	0.62	1.22	1.937	4.0
0.1000	0.70	0.90	2.592	3.7
0.0667	0.78	0.62	3.589	3.7
0.0500	0.83	0.49	4.592	3.5
0.0400	0.86	0.40	5.599	3.5
0.0333	0.88	0.34	6.609	3.5
0.0250	0.91	0.26	8.629	3.5
0.0125	0.949	0.133	16.74	3.5
0.0050	0.979	0.054	41.06	3.5
0.0025	0.990	0.027	81.12	3.4

TABLE II. Values of p_c, n_c, k, and $\langle A_{ex} \rangle$ are listed for ellipses with *two allowed orientations*. The value of k is obtained by evaluating the excluded area $\langle a_{ex} \rangle$ numerically and then using Eq. (6). The values of n_c are from simulation with the area of the ellipses fixed at $\pi/8$ and $\langle A_{ex} \rangle$ are obtained by using Eq. (4). The error bar in $\langle A_{ex} \rangle$ is ± 0.2.

b/a	p_c	n_c	k	$\langle A_{ex} \rangle$
1.0000	0.33	2.8	1.000	4.4
0.9000	0.33	2.8	1.002	4.4
0.8000	0.33	2.8	1.009	4.4
0.7000	0.34	2.7	1.024	4.3
0.6000	0.36	2.6	1.049	4.3
0.5000	0.37	2.5	1.091	4.3
0.4000	0.41	2.3	1.162	4.2
0.3333	0.45	2.06	1.237	4.0
0.2500	0.50	1.80	1.391	3.9
0.2000	0.54	1.59	1.548	3.9
0.1500	0.62	1.24	1.812	3.5
0.1000	0.68	0.97	2.342	3.6
0.0667	0.78	0.65	3.137	3.2
0.0500	0.82	0.51	3.933	3.2
0.0400	0.85	0.42	4.729	3.1
0.0333	0.87	0.37	5.525	3.2
0.0250	0.90	0.28	7.117	3.1
0.0125	0.947	0.145	13.48	3.1
0.0050	0.976	0.061	32.58	3.1
0.0025	0.989	0.028	64.41	2.8

For ellipses that can only lie in two directions, we see from Table II that

$$2.8 \leq \langle A_{ex} \rangle \leq 4.4 \ . \tag{5b}$$

Taking account of the error bars noted in the table captions, both these sets of results for $\langle A_{ex} \rangle$ are probably monotonic in the aspect ratio.

The excluded area of two identical ellipses can be defined as

$$\langle a_{ex} \rangle = 4\pi abk \ , \tag{6}$$

where k is a geometric factor that is chosen as above so that $k=1$ for circles. For randomly centered and oriented ellipses,[23]

$$k = \tfrac{1}{2} + s^2/8\pi^2 ab \ , \tag{7}$$

where s is the perimeter of an ellipse (this involves an elliptical integral which can be evaluated numerically). For randomly centered ellipses that can only lie in the two principal directions, the k factor is different from (7) and not available in a closed form for general b/a. For parallel ellipses $k=1$ but must be computed (using, for example, the contact function described in Sec. III) for ellipses at right angles. These two results are then averaged. The values of k for both these cases have been calculated and are given in Tables I and II for various aspect ratios.

From Eqs. (2), (4), and (6), we notice that

$$p_c = \exp(-\langle A_{ex} \rangle /4k) \tag{8}$$

which reduces to $p_c = \exp(-\langle A_{ex} \rangle /4)$ for circles when $k=1$.[16–18] In the *needle limit* where b/a is small and the ellipses are randomly oriented, using (7) we have $s=4a$ and $k=2a/\pi^2 b$, so that from Eq. (8)

$$p_c = \exp(-3.4/4k) = \exp(-0.425\pi^2 b/a) \approx 1 - 4.2b/a \ , \tag{9}$$

where we have used $\langle A_{ex} \rangle \approx 3.4$ from Table I. We note that in this limit, the result (9) is *independent of the precise shape of the needles*. For example, they can be elliptical or rectangular. As b/a becomes very small, only a few needles are needed to cross the sample, and these have essentially no area so that $p_c \to 1$ as given by (1). A similar limit is obtained for needles that can only point horizontally or vertically for which $k = a/(2\pi b)$. Using Eq. (8) with $\langle A_{ex} \rangle \approx 2.8$ from Table II, we find that

$$p_c = \exp(2.8/4k) = \exp(-1.4\pi b/a) \approx 1 - 4.4b/a \tag{10}$$

which we notice is close to the result for randomly oriented ellipses given in (9). Indeed because the values of $\langle A_{ex} \rangle$ are only known numerically, the error bars are sufficiently large that Eqs. (9) and (10) could be identical.

III. COMPUTER SIMULATIONS AND RESULTS

In our computer simulations, the whole system has periodic boundary conditions in both the x and y direc-

tions. For each fixed aspect ratio b/a about 2000 elliptical laminae are randomly distributed. The relative orientations are also random. An example of the system under study is shown in Fig. 1. As b/a becomes smaller fewer ellipses, for a given system size, are needed at percolation. To insure consistent statistics, we expanded the system size, while maintaining about the same number (2000) of ellipses. We determined n_c by keeping a record of whether there are clusters formed by overlaping elliptical laminae which cross the lower and upper boundaries at the same place (because of the periodic boundary condition).

In the course of recording clusters we used a very efficient algorithm involving a *contact function*[24] to determine whether two ellipses with given centers and relative orientation overlap or not. For two identical ellipses one centered at the origin and one centered at (x_0,y_0) with relative orientation θ, the contact function ψ is defined by

$$\psi=4(g_1^2-3g_2)(g_2^2-3g_1)-(9-g_1g_2)^2 , \tag{11}$$

where

$$g_1=3+(a/b-b/a)^2\sin^2\theta-(x_0/a)^2-(y_0/b)^2 , \tag{12}$$

$$g_2=3+(a/b-b/a)^2\sin^2\theta -(x_0\cos\theta+y_0\sin\theta)^2/a^2 -(y_0\cos\theta-x_0\sin\theta)^2/b^2 . \tag{13}$$

If ψ is negative, the two ellipses overlap. If ψ is positive and both g_1 and g_2 are positive, the two ellipses also overlap; otherwise the two ellipses do *not* overlap. If $\psi=0$, the two ellipses just touch. We only test those ellipses whose centers lie within $2a$ of each other. We find the average number of ellipses required for the system to percolate in both the x and y directions if (as invariably happens) one direction percolates before the other. Then we average over 25 to 30 samples for a fixed aspect ratio b/a and use Eq. (2) to evaluate p_c. The errors are due to the statistical averaging over the p_c which have a roughly Gaussian distribution. We repeat the same procedure for different aspect ratios b/a that range from $\frac{1}{400}$ up to 1.0.

In Fig. 2 the percolation threshold p_c is plotted against the aspect ratio b/a. The results for both randomly oriented ellipses and ellipses that are aligned along two perpendicular directions are shown. It can be seen that the two sets of results are indistinguishable within our limits of accuracy.

We have also evaluated $\langle A_{ex}\rangle$ using n_c found from the computer simulation and Eqs. (4) and (6) for both randomly oriented and two-direction-oriented ellipses. The error bar in our computer simulation in determining n_c is about $\pm5\%$; therefore the error bar in $\langle A_{ex}\rangle$ is about ±0.2. Tables I and II list p_c, n_c, k, and $\langle A_{ex}\rangle$ for various aspect ratios b/a for the two cases and they show that in both cases $\langle A_{ex}\rangle$ decreases very slowly as b/a decreases.

In the following discussion, we only consider quantities for the randomly oriented case. The case of only two orientations would give essentially indistinguishable results. Note that although n_c and hence p_c are virtually indistinguishable for a fixed aspect ratio b/a in the two

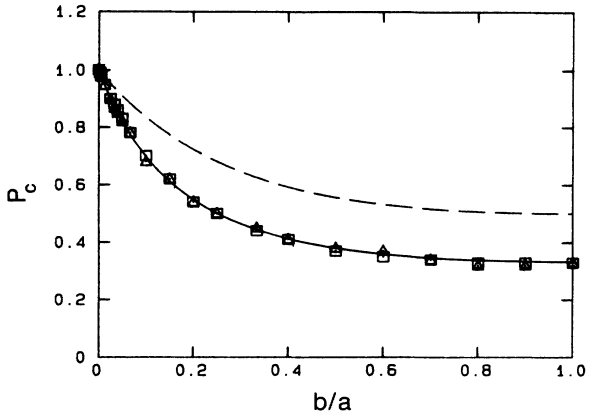

FIG. 2. Percolation threshold p_c for various aspect ratios b/a. □ denote randomly oriented ellipses, while △ denote vertically and horizontally oriented ellipses. Every point is averaged over 25–30 samples each containing ~2000 ellipses. The solid curve is the interpolation formula (27) for p_c. The dashed curve is p_I, which gives the initial slope for the conductivity from Eq. (22).

cases, the quantities k and $\langle A_{ex}\rangle$ are different as can be seen by comparing Tables I and II.

In Fig. 3 we plot $f_1=\pi abn_c$ and $f_2=1-f=1-\exp(\pi abn_c)$. The quantity f_1 is the total area in the ellipses for a sample of unit area, not allowing for the overlap effects, whereas f_2 is less than f_1 because overlap effects are included. It can be seen that for small b/a these two quantities are the same, as the overlap area for needles is negligibly small. In the circle limit $f_1=1.09\pm0.02$; that is, the area in the circles at percolation, before they are thrown down, is greater than unity. Note that if f_2 is expanded in powers of the density n_c, the first term is f_1 and the corrections for r body overlap are given by the coefficient of the n_c^r term.

IV. CRITIQUE OF EFFECTIVE-MEDIUM THEORIES

There are extensive discussions in the literature on EMT for dielectric constants[3] and elastic moduli[11] of

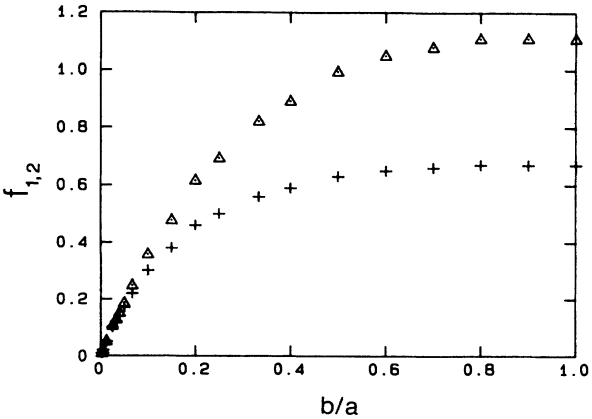

FIG. 3. Quantities $f_2=1-\exp(\pi abn_c)$ and $f_1=\pi abn_c$ are plotted against the aspect ratio b/a for the case of randomly oriented ellipses. + denote f_2 and △ denote f_1.

composite materials with circular or spherical inclusions. A strong assumption is always required in deriving these approximations that the inclusion concentration is sufficiently low that interference effects can be neglected. However, these approximations are often used over the whole concentration range where they are of dubious validity. In order to judge how good various EMT results are when applied to completely permeable objects, we see how close their predictions of p_c are compared to our exact (numerical) results. Physical properties, like the conductivity and all elastic moduli, should vanish at p_c when holes are punched in the medium. Similarly, the resistance and all the elastic compliances should vanish when infinitely hard inclusions are present in the medium. Infinitely hard means superconducting in the electrical case and infinitely rigid or undeformable in the elastic case. All these p_c should be the same as it is a geometrical property of the material. However, different EMT give very different estimates for p_c. These various EMT predictions for p_c can be used as a figure of merit, when compared to our exact results, to judge how good the EMT is away from the dilute limit. In what follows we will examine two versions of EMT for each physical property. Depending on whether we treat the inclusion and background symmetrically or asymmetrically, two versions (i.e., symmetric or asymmetric) of EMT can be derived.[3] Thus we have *eight cases to consider,* electrical or elastic, symmetric or asymmetric with inclusions that are either holes (Swiss-cheese model) or hard inclusions (reinforced model). Sen, Thorpe, and Milton[6] have summarized these results for the electrical case. These results can also be obtained from Ref. 3. The critical p_c for the dilute (Swiss-cheese) case are

$$p_c^s=\tfrac{1}{2}\ , \tag{14}$$

$$p_c^a=(a^2+b^2)/(a+b)^2\ , \tag{15}$$

where the superscripts s and a refer to the symmetric and asymmetric cases, respectively. The results for the reinforced case are identical to (14) and (15). Similar results have been obtained by Thorpe and Sen[7] for the elastic case. For the dilute (Swiss-cheese) model, all the elastic moduli vanish at

$$p_c^s=2\{1+[2(a+b)^2/(a^2+b^2)]^{1/2}\}^{-1}\ , \tag{16}$$

$$p_c^a=[1+ab/(a^2+b^2)]^{-1}\ . \tag{17}$$

For the reinforced model, all the elastic compliances vanish at

$$p_c^s=1-2\{1+[2(a+b)^2/(a^2+b^2)]^{1/2}\}^{-1}\ . \tag{18}$$

$$(1-p_c^a)^{-1}=2\{1+(1-\sigma)(a+b)^2/[2ab(1+\sigma)]\}/(3-\sigma)$$

$$=(1-p_c^a)^{-1}=\{(a+b)^2/[ab(3-\sigma)]+1/[1-ab(1+\sigma)/(a+b)^2]\}/2\ , \tag{19}$$

where p_c^a is found from Eq. (19) by eliminating σ, the value of Poisson's ratio at the critical point. If these were exact theories, all the results (14)–(19) would be identical. Note that there is no difference between the symmetric and asymmetric cases in the circle limit for all these results. The above results are shown in Fig. 4 as a function of the aspect ratio, and we can see that only curve 6 which is the result (19) is reasonable. Indeed all results except for the reinforced elastic model fail to get even the circle limit correct. These two approximations for the reinforced elastic model [Eqs. (18) and (19)] give $p_c=\frac{1}{3}$ which is the correct result for circles within numerical error as can be seen from Tables I and II. These results show that EMT is inadequate, when strong disorder is present, except in the one special case. In other cases we believe a better procedure is to develop *interpolation* formulas.

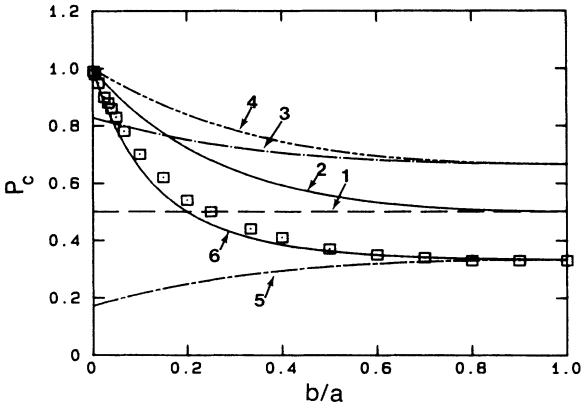

FIG. 4. Percolation thresholds p_c predicted from various effective-medium theories and our computer simulations from Fig. 2. The curves are marked 1 for Eq. (14), 2 for Eq. (15), 3 for Eq. (16), 4 for Eq. (17), 5 for Eq. (18), and 6 for Eq. (19). ⊡ indicate the exact percolation thresholds from computer simulations taken from the results for randomly oriented ellipses in Fig. 2.

We note that Eq. (19) could be used as a useful parametric approximation to p_c when required. It gives $p_c=\frac{1}{3}$ (compared with 0.33 in Tables I and II) in the circle limit and

$$p_c\approx 1-\tfrac{16}{3}(b/a) \tag{20}$$

in the needle limit. This should be compared with Eqs. (9) and (10)

V. INTERPOLATION FORMULAS

As we mentioned in the Introduction, the Clausius-Mossotti equation for the conductance of a two-phase system is exact when one phase has a very low concentration. All attempts to extend these equations beyond this region are rather uncontrolled and many versions exist in

the literature. As we discussed in the previous section, all are unsatisfactory for the electrical case. We therefore develop a simple interpolation formula that gets all the known limits for the dilute (Swiss-cheese) model correct. We believe that this should be of considerable utilitarian use. Similar formulas can be written down for other cases.

For a *small* number of holes in a material with conductance Σ_0 the effective conductance Σ is given by

$$\Sigma=\Sigma_0[1-(1-p)/(1-p_I)] , \tag{21}$$

where

$$p_I=(a^2+b^2)/(a+b)^2 . \tag{22}$$

The quantity p_I is where the *initial* slope for a small number of defects[3,6] would eventually cross the $\Sigma=0$ axis when *extrapolated* and is a convenient way to express the initial slope. The relation $\Sigma\sim(p-p_c)^t$ holds only in the small critical region around p_c. Our interpolation formula is designed to link these two limits by assuming the conductivity has the following form:

$$\Sigma=\Sigma_0(1.0+\alpha c+\beta c^2)^\lambda , \tag{23}$$

where $c=1-p$ and α, β, and λ are constants to be determined from the following:

$$\Sigma\sim(p-p_c)^t \text{ as } p\to p_c , \tag{24}$$

$$\Sigma=\Sigma_0[1-c/(1-p_I)+O(c^2)] \text{ as } c\to 0 , \tag{25}$$

and Σ_0 is the conductivity of the sample without any inclusions ($c=0$). Of course one would like to include higher-order terms in c in Eq. (23), but since we have no more information other than (24) and (25), it is not possible to do better. After some simple algebra we find

$$\Sigma/\Sigma_0=\{1-c/[t(1-p_I)]-c^2[t(1-p_I)-(1-p_c)]/[t(1-p_I)(1-p_c)^2]\}^t . \tag{26}$$

It is rather inconvenient to use the expressions (19) for p_c and so we make a simpler approximation (27) for p_c that is correct in the two limits $b/a=1$, when $p_c\approx\frac{1}{3}$ and b/a small, when $p_c\approx 1-\frac{9}{2}(b/a)$ from Eqs. (9) and (10):

$$p_c=(1+4y)/(19+4y) , \tag{27}$$

where $y=b/a+a/b$ is symmetric in $a\leftrightarrow b$. The result (27) is virtually indistinguishable from the computer simulations in Fig. 2 and is actually *superior* to (19) as can be seen by comparing Figs. 2 and 4. Of course there is no rigorous basis for (27) except that it fits the simulation data for all aspect ratios.

By taking $t=1.3$,[1] and using Eq. (22) for $p_I=y/(2+y)$ and Eq. (27) for p_c, we can determine the effective conductance Σ,

$$(\Sigma/\Sigma_0)^{1/t}=1-c(2+y)/(2t)+c^2(19+4y)[9(2+y)-(19+4y)t]/(324t) , \tag{28}$$

which we recommend for use in practice (with $t=1.3$) as it reproduces all the presently known results (i.e., the value of Σ for the pure system, with $p=1$; the initial slope for small $1-p$; the value of $p=p_c$ where Σ vanishes with critical exponent t) to within numerical accuracy. Note that the term in c^2 is always small and positive. This is because p_I is always larger than p_c for all aspect ratios ($1\le p_I/p_c\le 1.5$) as can be seen from Fig. 4. In Fig. 5, Σ/Σ_0 is plotted against $p=1-c$ for various aspect ratios b/a and shown as the solid lines. Also in Fig. 5, Σ/Σ_0 is plotted against c but with $t=1.0$ for the same aspect ratios and shown as the dashed line. The two plots are quite similar and only differ a little in the critical region. Clearly the EMT described in Sec. IV would give very different results as the p_c are so different.

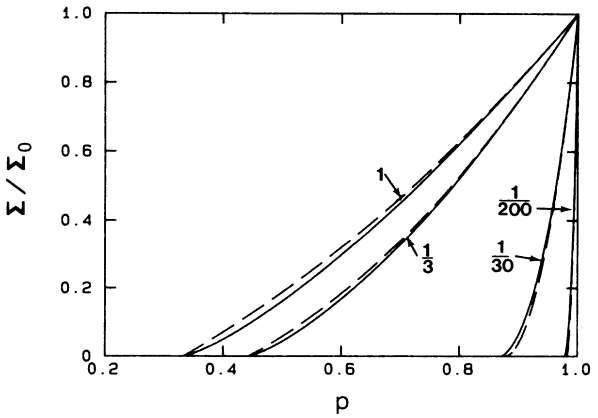

FIG. 5. Electrical conductance from the interpolation formula (28) for various aspect ratios as indicated. The solid curves are for $t=1.3$ and the dashed curves are for $t=1.0$.

Because of the equivalence of the problems, the interpolation formula (28) can be used for the *electrical conductivity* of sheets containing holes, the *thermal conductivity* of sheets containing holes, or the the *dielectric constant* of a medium with holes. In all cases, $p=1-c$ is the fraction of material remaining after the holes have been punched and $y=b/a+a/b$, where b/a is the ratio of the minor-to-major axis of the ellipses.

If the inclusions are *superconducting* rather than insulating (i.e., holes), then the result (28) still holds if we replace Σ/Σ_0 on the left-hand side with R/R_0, where R is the resistance of the sample and R_0 is the resistance when there are no inclusions ($c=0$). These two problems map onto one another and are exactly equivalent.[25,26] Note that p_I and p_c given in Eqs. (22) and (27) and the critical exponents are the same.[1,3]

Finally we note that the interpolation formula (28) has two interesting limiting forms. Using the limiting forms

for p_I and p_c, we find that for circles,

$$(\Sigma/\Sigma_0)^{1/t}=1-2c/t+3c^2(4-3t)/4t \ , \tag{29}$$

and for needles,

$$(\Sigma/\Sigma_0)^{1/t}=1-n\pi L^2/8t+n^2\pi^2L^4(9-4t)/1296t \ , \tag{30}$$

where we have used Eq. (1) with $A=\pi ab$ and put $c=1-p=1-\exp(-\pi abn)\approx n\pi ab$ and the length of the needles is $L=2a$. The result (30) is independent of the width b of the needles as would be expected. Here n is the number of inclusions per unit area.

VI. SUMMARY OF RESULTS

Our main result has been the numerical determination of the percolation concentration of randomly centered and oriented ellipses. This has been done by using a contact function to determine if neighboring ellipses overlap and constructing a connectivity table. It is not necessary to measure any overlap areas to find the areas at percolation; it is sufficient to merely count the number of ellipses. We have also determined the percolation concentration of ellipses when the axes are constrained to lie in only *two* Cartesian directions. The results are indistinguishable, within our numerical accuracy, from the previous case where all orientations are allowed.

We have used these results to critique various effective-medium theories that have been developed for the electrical and elastic responses of sheets containing elliptical inclusions. Only one of these approximations is found to give a reasonable percolation threshold while all the others fail to describe the electrical conductivity or elastic properties near the critical point.

We have shown that the *percolation concentration* is described well by the formula $p_c=(1+4y)/(19+4y)$, where $y=b/a+a/b$. Here p_c is the amount of material *remaining* and b/a is the aspect ratio of the ellipses. We have also developed a simple interpolation formula for the *electrical conductance* that is correct both for a few inclusions and near percolation. We believe this kind of formula is superior to effective-medium theories and may have useful practical applications.

ACKNOWLEDGMENTS

We should like to acknowledge many interesting and useful conversations with S. de Leeuw, E. Garboczi, and P. Sen. The financial support of the U.S. Office of Naval Research under Grant No. N00014-80-C-0610, the Michigan State University Center for Fundamental Materials Research, and NATO is gratefully acknowledged.

*Present address: Department of Physics and Astronomy, Rutgers University, Piscataway, NJ 08855.

[1]B. I. Halperin, S. Feng, and P. N. Sen, Phys. Rev. Lett. **54**, 2391 (1985).

[2]C. J. Lobb and M. G. Forrester, Phys. Rev. B **35**, 1899 (1987).

[3]R. Landauer, in *Electrical Transport and Optical Properties of Inhomogeneous Media (Ohio State University, 1977)*, Proceedings of the First Conference on the Electrical Transport and Optical Properties of Inhomogeneous Media, AIP Conf. Proc. No. 40, edited by J. C. Garland and D. B. Tanner (AIP, New York, 1978).

[4]R. I. Cukier, J. Phys. Chem. **89**, 246 (1985).

[5]S. Kirkpatrick, in *Ill-Condensed Matter, Les Houches 1978*, proceedings of the conference, edited by R. Balian, R. Maynard, and G. Toulouse (North-Holland, Amsterdam, 1979).

[6]P. N. Sen, M. F. Thorpe, and G. Milton (unpublished).

[7]M. F. Thorpe and P. N. Sen, J. Acoust. Soc. Am. **77**, 1674 (1985).

[8]R. Hill, J. Mech. Phys. Solids **13**, 213 (1965); B. Budiansky, *ibid.* **13**, 223 (1965).

[9]T. T. Wu, Int. J. Solids Struct. **3**, 1 (1966).

[10]J. Berryman, J. Acoust. Soc. Am. **68**, 1820 (1980), and references therein.

[11]J. P. Watt, G. F. Davies, and R. J. O'Connell, Rev. Geophys. Space Phys. **14**, 541 (1976).

[12]I. Balberg, Phys. Rev. B **31**, 4053 (1985).

[13]D. Stauffer, *Introduction to Percolation Theory* (Taylor and Francis, London, 1985).

[14]L. N. Smith and C. J. Lobb, Phys. Rev. B **20**, 3653 (1979).

[15]F. Carmona and A. El Amarti, Phys. Rev. B **35**, 3284 (1987).

[16]A. S. Skal and B. I. Shklovskii, Fiz. Tekh. Polyprovdn. **7**, 1589 (1973) [Sov. Phys. Semicond. **7**, 1058 (1973)].

[17]V. K. S. Shante and S. Kirkpatrick, Adv. Phys. **20**, 325 (1971); G. E. Pike and C. H. Seager, Phys. Rev. B **10**, 1421 (1974).

[18]C. Mark, Proc. Cambridge Philos. Soc. **50**, 581 (1954).

[19]We list here the results for p_c for circles with references: $p_c=0.325$ (Ref. 17), $p_c=0.32\pm0.02$ (Ref. 18), $p_c=0.33\pm0.02$, D. H. Fremlin, J. Phys. (Paris) **37**, 813 (1976); $p_c=0.324\pm0.002$, E. T. Gawlinski and H. E. Stanley, J. Phys. A **14**, L129 (1981); $p_c=0.322\pm0.005$, T. Vicsek and J. Kertesz, *ibid.* **14**, L31 (1981).

[20]I. Balberg, C. H. Anderson, S. Alexander, and N. Wagner, Phys. Rev. B **30**, 3933 (1984).

[21]L. Onsager, Ann. N.Y. Acad. Sci. **51**, 627 (1949).

[22]R. Zallen, *The Physics of Amorphous Solids* (Wiley, New York, 1983).

[23]A. S. Roach, *Theory of Random Clumping* (Spottiswoode and Ballantyne, London, 1968).

[24]J. V. Baron, J. Chem. Phys. **56**, 4730 (1972).

[25]J. B. Keller, J. Math. Phys. **5**, 548 (1964).

[26]K. S. Mendelson, J. Appl. Phys. **46**, 917 (1974).